Original Research

Changes in islet microvasculature following streptozotocin-induced β-cell loss and subsequent replacement in the neonatal rat

J Michael Nicholson[1,4], Edith J Arany[1,2,3] and David J Hill[1,2,4,5]

[1]Lawson Health Research Institute, St Joseph's Health Care, London, Ontario, Canada N6A 4V2; [2]Department of Medicine; [3]Department of Pathlogy; [4]Department of Physiology and Pharmacology; [5]Department of Paediatrics, University of Western Ontario, London, Ontario, Canada N6A 5B8

Corresponding author: David J Hill, Lawson Health Research Institute, St Joseph's Health Care, 268 Grosvenor St, London, Ontario, Canada N6A 4V2. Email: dhill@lri.sjhc.london.on.ca

Abstract

Neonatal rats undergo considerable β-cell regeneration after depletion with streptozotocin (STZ). Since the intraislet vasculature is necessary for both β-cell growth and function, we examined changes in vascular morphology following STZ. Neonatal Wistar rats (4 days) were injected with 70 mg/kg STZ, or buffer, and were examined between days 4 and 40 postinjection. Animals receiving STZ were relatively hyperglycemic for eight days, but became normoglycemic subsequent to a partial recovery of β-cell mass. However, glucose tolerance remained impaired. The intraislet area occupied by capillaries was significantly reduced by approximately 20% following STZ, mainly within the β-cell-rich islet core, but had recovered by day 40. Vascular endothelial growth factor (VEGF) was localized to β-cells, and pancreatic VEGF mRNA levels in control animals showed a progressive increase between days 4 and 20. This rise was delayed following STZ, but by day 20 VEGF mRNA abundance exceeded that in control pancreas. Hepatocyte growth factor (HGF) was localized to intraislet endothelial cells. Levels of HGF mRNA increased until day 16 in control rats, but subsequently declined to low levels. Following STZ, HGF mRNA had declined prematurely after day 12. Type IV collagen was localized to the extracellular matrix around the intraislet vasculature. The islet area immunopositive for collagen was significantly reduced at all times following STZ. Results indicate that there is a relative loss of intraislet vasculature following STZ, which may limit subsequent β-cell regeneration through both local growth factor and extracellular matrix interactions.

Keywords: neonatal rat, streptozotocin, endothelial cell, VEGF, HGF

Experimental Biology and Medicine 2010; **235**: 189–198. DOI: 10.1258/ebm.2009.009316

Introduction

The extensive vascular architecture of the islet is important for optimal β-cell function and the export of insulin. However, the intimate relationship between the β-cell and neighboring endothelial cells (ECs) dates back to embryonic and fetal development, where the appearance of endocrine tissue within the pancreas occurs concurrently with microvessel development.[1] Juxta positioning of the developing vasculature and primitive gut endoderm at E8.5–E10.5 in the mouse embryo causes the appearance of the pancreatic buds that will ultimately form the head and tail of the pancreas, and the expression of pancreatic and duodenal homeobox 1 in the endoderm, a transcription factor necessary for pancreatic endocrine cell lineage commitment.[2]

The intimate interdependence between vasculature and β-cells extends into postnatal life where ECs forming the rich microvasculature within the islets are uniquely adapted to maintaining both growth and function of the β-cells.[3] The islet ECs are highly fenestrated allowing for rapid export of insulin, while phage display showed that more than 80% of the cell membrane receptors present differed from those present on ECs from pancreatic exocrine tissue.[4,5] Intraislet vessels provide a basement membrane for β-cells that is rich in laminin and type IV collagen, and ECs have been demonstrated to promote β-cell proliferation and function via the release of soluble growth factors, such as hepatocyte growth factor (HGF), and integrin signalling across the shared basement membrane.[6–10] A reciprocal signalling from the β-cell to promote EC proliferation is achieved through the secretion of vascular endothelial growth factor (VEGF) and insulin, the former being responsible for the high degree of capillary fenestration seen in the islets.[6,11]

Regeneration of β-cell mass following chemical or surgical ablation has been widely studied in rodent models. In rats, extensive remodelling of islets occurs in the neonatal period involving β-cell turnover and the generation of new islets by neogenesis.[12] Administration of streptozotocin (STZ) to the neonatal rat results in rapid β-cell loss, but animals can rapidly regain glycemic control and β-cell mass will largely recover over several weeks.[13–17] Approximately 50–60% of the β-cell regeneration is derived by replication of remaining β-cells and the balance is most probably contributed by neogenesis of new islets from the pancreatic dusts. The immediate stimulus to enhance β-cell proliferation following STZ-induced loss is unclear, as is the involvement of the islet vasculature. Bone marrow-derived endothelial precursor cells can infiltrate the STZ-damaged islets and can induce β-cell regeneration.[18] This does not involve a widespread transdifferentiation into a β-cell phenotype, but is associated with the differentiation of endocrine precursor cells into ECs that can incorporate into islet capillaries.[19,20] The vasculogenesis may then induce proliferation in adjacent β-cells through paracrine signalling.

The hypothesis underlying this study was that anatomical and functional changes may occur within the islet microvasculature following administration of STZ to the neonatal rat due to the loss of functional interaction with β-cells that have been destroyed. We anticipated that any changes in the islet microvasculature would subsequently be linked to the capacity for β-cell regeneration.

Methods

Animals

Wistar rats (Charles River, St Constant, PQ, USA), weighing between 200 and 250 g were acclimatized for a minimum of five days, provided with a 12-h dark, 12-h light cycle and access to water and standard rodent chow before mating. The offspring were allowed to deliver naturally. On day 4 of neonatal life, rats were randomly allocated to one of two groups: a control group that was given an intraperitoneal bolus injection of vehicle consisting of 100 μL/g bodyweight, 0.1 mmol/L (pH 4.5) citrate buffer (vehicle) or a β-cell-depleted group that was given an intraperitoneal bolus injection of 70 mg/kg (body weight) STZ in vehicle. Animals were killed on the fourth day postinjection by decapitation, and then every fourth day thereafter until days 20 and 40 by CO_2 asphyxiation. Five or six pups, each from a separate litter, were collected for study at each time point. At sacrifice the body weight was recorded and pancreata were collected immediately, weighed and fixed for histology or preserved in RNAlater® solution (Applied Biosystems, Streetsville, ON, USA) and then stored at −80°C for future RNA quantification.

To ensure that the STZ injection caused β-cell destruction, glucose levels were measured in both control and STZ-treated pups after a two-hour fast two days postinjection.[13] The fasting blood glucose was also measured after a four-hour fast prior to sacrifice at each time point studied. One control and one STZ-treated animal from the same litter were subjected to an intraperitoneal glucose tolerance test (IPGTT) for nine separate litters. The IPGTT was performed on days 10 and 40 postinjection when a bolus of intraperitoneal glucose (2 g/kg body weight) was given after a five-hour fast. Blood was sampled from the tail vein for up to two hours for glucose measurement. All procedures were performed with the approval of the ethics committee of the University of Western Ontario, and in accordance with the guidelines of the Canadian Council on Animal Care.

Immunohistochemistry

Tissue was fixed in 10% buffered formalin (VWR Laboratories, West Chester, PA, USA) (pH 7.4) for 24–36 h before embedding in paraffin. Sequential sections of 5 μm were cut over 100 μm from the head region of the pancreas and were individually mounted onto SuperFrost Plus glass slides (Fisher Thermo Scientific, Nepean, Ontario, Canada). After omission of the next 200 μm of each block, a further 50 μm were cut at 5 μm and mounted. These sections were then stored at room temperature until analysis.

Immunohistochemistry was performed to localize insulin, proliferating cell nuclear antigen (PCNA) using guinea pig anti-insulin (1:300 dilution, Abcam, Mississauga, Ontario, Canada) and mouse anti-PCNA (1:100, Sigma-Aldrich, St Louis, MO, USA), respectively. Islet blood vessels were visualized using a biotinylated lectin from the bacteria *Bandeiraea simplicifolia* lectin (BS-l) (1:30 dilution, Vector Laboratories, Burlington, Ontario, Canada), a specific glycosylated protein on rodent ECs.[14,21,22] BS-l lectin is specific for ECs and is not present on other islet cell types. Sections were deparaffinized and blocked with 5% (v/v) goat and horse serum for 30 min at room temperature. All antibodies were diluted in antibody diluent (Dako, Mississauga, Ontario, Canada). Slides were incubated with the primary antibody for PCNA, or biotinylated BS-l, each for 24 h, in a humidified chamber at 4°C, and with the anti-insulin antibody for one hour at room temperature. Biotinylated goat anti-guinea pig and horse anti-mouse were used as secondary antibodies. Signal amplification and visualization were accomplished by incubation with either peroxidase-conjugated extravidin labelling reagent (Sigma-Aldrich) and 3,3′-diaminobenzidine tetrahydrochloride (DAB) substrate pack (Biogenex, Markham, Ontario, Canada), which yields a brown (insulin) product, or an avidin–biotin complex solution (Vectastain ABC Elite, Vector Laboratories) with visualization using alkaline phosphatase, with red (BS-l) and blue (PCNA) (alkaline phosphatase substrate kit III, Vector) reaction products as the chromogens. Sections were mounted under glass cover slips with VectaMount® (Vector Laboratories). Laminin co-localization was performed using the same protocol described using rabbit anti-laminin antiserum (1:50, Fisher Thermo Scientific) in place of the conjugated BS-l. HGF and collagen type IV staining were performed using a rabbit anti-HGF (1:30 dilution, Santa Cruz Biotechnology, Santa Cruz, CA, USA) or rabbit anti-collagen (1:50 dilution, Abcam) as described above using DAB substrate. A sequential section was used to stain for BS-l to identify the islet cells involved with HGF production.

For dual immunofluorescent localization of insulin and VEGF, sections were deparaffinized and blocked as described above. A mixture containing guinea pig anti-insulin and rabbit anti-VEGF (1:50 dilution, Abcam) was then added to the sections and incubated for one hour at room temperature. After washing for 10 min in phosphate-buffered saline (PBS), a mixture of secondary antibodies was added consisting of goat anti-rabbit (Alexa Fluor 555, 1:200 dilution, Molecular Probes, Eugene, OR, USA) and goat anti-guinea pig (Alexa Fluor 488, 1:200 dilution, Molecular Probes) for 30 min. Nuclei were co-localized by the staining of DNA with 4′6-diamidino-2 phenylindole (Sigma-Aldrich). The sections were washed in PBS and mounted using Vectashield® mounting medium for fluorescence (Vector Laboratories).

Controls included omission of primary antisera, omission of secondary antibody or absence of staining after preincubation of the antiserum with excess antigen (insulin, HGF and VEGF), as described previously.[14]

Morphometric analysis

Pancreata from at least five separate litters of rats were examined using three representative sections of the head of the pancreas, at each time point. Images were obtained by light microscopy at magnifications of ×200 or ×400. All analyses were performed using Northern Eclipse morphometric analysis software (Empix Imaging, version 7.0, Mississauga, Ontario, Canada) and verified by a 'blinded' observer. All islets above 500 μm^2 area were analyzed and counted in the entire section of pancreas excluding any extraislet endocrine cells. To determine the size of an islet, the surrounding basement membrane was traced. Islet blood vessels were traced to include the lumen. The percentage of islet area occupied by vessels, and the insulin-positive cell area per mm^2 were calculated for each group between days 4 and 20, and at day 40. To estimate β-cell mass, the total area occupied by insulin-immunoreactive cells was calculated and expressed relative to the total sectional area of pancreas. This was then expressed per mg based on the total weight for that pancreas, as described previously.[23]

The number of insulin-positive cells that also demonstrated nuclear staining for PCNA was expressed as a percentage relative to the total number of insulin-positive cells in the same section. These double-labelled cells were then analyzed by relative location to islet vessels, adjacent or non-adjacent. Islet blood vessels with ECs that also showed nuclear staining for PCNA were expressed as a percentage of the total number of vessels in an islet. Analyses were audited for bias by allocating a sample of the determinations to a blinded observer.

RNA isolation and reverse transcription

Total RNA was isolated from whole pancreata and purified following the RNeasy Plus Minikit (Qiagen, Mississauga, Ontario, Canada) protocol before being re-suspended in ultrapure distilled DNAse/RNAse-free water (Invitrogen Canada, Burlington, Ontario, Canada). Each preparation of RNA was assessed for degradation by separation on 1.5% denaturing agarose gel. Only if 18S and 28S ribosomal RNA bands were clearly visible was the sample utilized further. RNA concentrations and quality were determined from spectrophotometric absorption at 260 nm, and the ratio of absorbance at 260/280 nm was assessed to confirm purity (ratios >1.9). Reverse transcription was performed using Superscript II (Invitrogen) following the manufacturer's instructions. Two micrograms of total RNA were reversed transcribed in a total volume of 20 μL using random hexomer primers (Invitrogen). For every reverse transcription (RT) reaction set, one RNA sample was setup without reverse transcriptase enzyme as a negative control. Reactions were incubated at 25°C for 10 min, 43°C for 90 min, 94°C for four minutes and then maintained at 4°C. After RT, samples were then diluted by addition of ultrapure distilled DNAse/RNAse-free water.

Realtime quantitative polymerase chain reaction

Realtime quantitative polymerase chain reaction (PCR) was performed using TaqMan probe technologies in an ABI Prism 7900HT sequence detection system (Applied Biosystems) to determine the relative abundance of VEGF-A (Rn00582935_m1) and HGF (Rn00566673_m1) using β-tubulin (Rn00597407_m1) as an endogenous control. These primer–probe sets each spanned an intron to achieve RNA specificity. PCR was run in triplicate 25 μL reactions that consisted of 7.25 μL of ultrapure distilled DNAse/RNAse-free water, 12.5 μL TaqMan Universal PCR MasterMix (Applied Biosystems), 1.25 μL Assays-on-Demand Gene Expression Assay Mix and 4 μL consisting of 100 ng cDNA. Two-step PCR cycling was carried out as follows: one cycle of 50°C for two minutes, one cycle of 95°C for 10 min and 45 cycles of 95°C for 15 s and 60°C for one minute. A validation experiment was performed on control tissue (day 4) to demonstrate that the efficiencies of target and reference genes were approximately equal. The log of input cDNA versus the comparative threshold (CT) value was plotted to determine if the line of best fit had an absolute slope <0.1. Three or four animals from separate litters were analyzed. The CT method (ΔΔCT) was used. The threshold cycle range for VEGF mRNA was 22–28; that for HGF mRNA was 26–33; and for β-tubulin was 20–27. A validation curve was produced and the line of best fit was produced using three ΔCT data points. The slope of the lines of best fit for VEGF and HGF were −0.0694 and −0.056, respectively.

Statistical analysis

All values are presented as mean ± standard error of mean. Statistical comparisons were performed using two-way analysis of variance, with the Bonferroni's *post hoc* test and $P < 0.05$ was considered to be the minimum for statistical significance. The areas under the curve (AUC) for glucose tolerance tests were compared using an unpaired Student's *t*-test. All experimental times are given as days following administration of STZ or buffer control. Chronological age is four days greater.

Results

Recovery of glycemic control and β-cell mass following STZ

The fasting blood glucose for animals injected with STZ was significantly increased ($P < 0.05$, $n = 12$) two days postinjection and relative hyperglycemia was observed at days 4 and 8 in STZ-treated animals versus controls (Table 1). Thereafter, control and STZ-treated rats had similar fasting blood glucose levels. An IPGTT performed 10 days post-STZ treatment (Figure 1a) showed that glucose tolerance was impaired compared with control animals, and remained so after 40 days (Figure 1b). Animals followed until adulthood at day 130 following STZ treatment still showed a relative impairment of glucose tolerance. Four days following administration of STZ, approximately 70% of β-cell mass was lost compared with control animals, but islet size and morphology with a central core of insulin-immunoreactive β-cells had recovered after 40 days (Figures 2a–d). When β-cell mass was quantified in pancreata following STZ treatment, this increased up to 40 days after the insult, but still represented only half the β-cell mass found in control rats of equivalent age (Figure 2e). The mean total number of islets per tissue section was not altered following STZ (not shown). When STZ-treated rats were observed as adults at 130 days, β-cell mass was still relatively deficient.

Islet blood vessels

Islet blood vessels were visualized using the bacteria BS-l, as shown on day 16 (Figures 3a and b) in pancreata from control and STZ-treated animals. Insulin and PCNA, indicative of cells undergoing DNA synthesis, were co-localized to the same tissue sections. BS-l identified ECs within the islets and acinar tissue, although acinar cells also showed weak intracellular staining. Within the islets, proliferating insulin-immunoreactive β-cells could also be identified. Calculation of the percentage area of islets occupied by capillaries (Figure 3c) showed that this was significantly reduced in islets from STZ-treated rats compared with controls between four and 16 days, and recovered at days 20 and 40. We also calculated the percent of islet capillaries that were present within the core of each islet, defined as the area of insulin-immunopositive β-cells. This remained constant in control rats at 80–85% between days 4 and 40 (Table 2). However, following STZ treatment this was reduced to less than 55%, and remained significantly below values for control animals until day 20, before recovering by day 40. It would appear that there is a relative loss of intraislet capillaries from the β-cell-rich islet core following STZ. No changes were found in capillary density in the exocrine tissue of the pancreas between control and STZ-treated animals at any time point.

We examined the rate of β-cell proliferation at three time points, days 12, 16 and 20, representing the time of commencement of recovery of β-cell mass following STZ. The percent of insulin-immunoreactive β-cells co-staining with PCNA was consistently elevated after STZ treatment (Figure 4a). The percentage of intraislet capillaries that contained at least one PCNA-immunoreactive EC was significantly higher on both days 16 and 20, when compared with day 12, in both the control and STZ-treated rats (Figure 4b). However, there was no difference between control and STZ groups at any time point.

Table 1 Mean fasting blood glucose in control rats or those treated with streptozotocin (STZ) between two and 40 days after treatment

	Fasting blood glucose (mmol/L)	
Day	Control	STZ
2	5.8 ± 1.3	8.0 ± 1.2*
4	5.8 ± 0.7	8.3 ± 1.2*
8	5.5 ± 0.6	7.1 ± 0.8*
10	5.6 ± 0.5	6.5 ± 0.8
12	5.5 ± 0.8	6.2 ± 1.2
16	5.8 ± 0.7	6.3 ± 1.2
20	5.8 ± 0.9	5.7 ± 1.2
40	6.2 ± 0.9	6.1 ± 1.4

Values show mean ± SD
*$P < 0.05$ versus control ($n = 12$ animals)

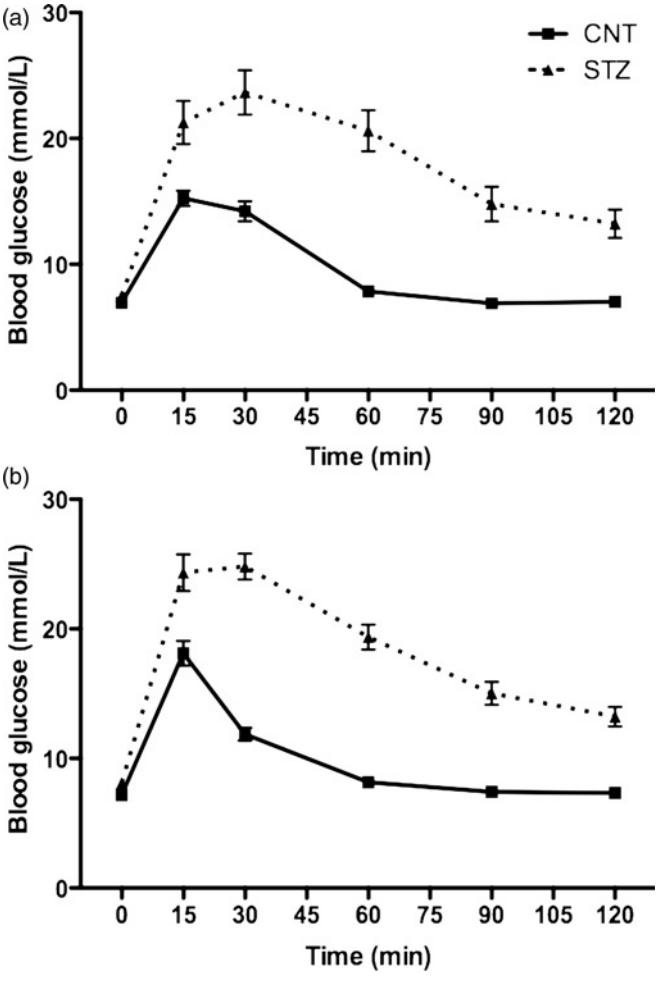

Figure 1 Glucose profile following an intraperitoneal glucose tolerance test in control (solid line) or STZ-treated (broken line) animals 10 days (a) or 40 days (b) after STZ or saline treatment. Data are presented as mean ± SEM. STZ, streptozotocin; CNT, control

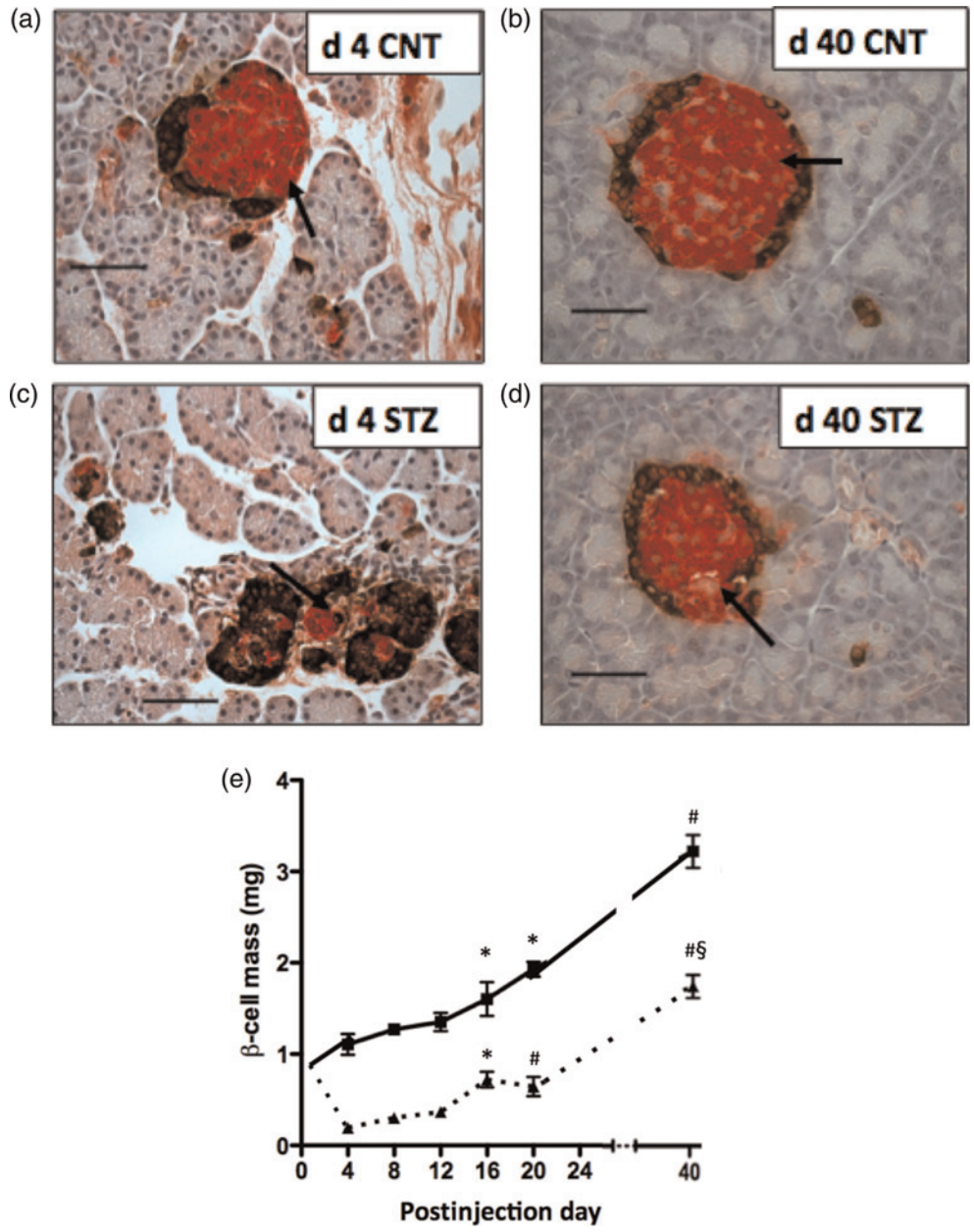

Figure 2 Islet morphology (arrows) in control (CNT) or streptozotocin (STZ)-treated animals day 4 (a and b) or day 40 (c and d) after treatment with STZ or saline. Immunohistochemistry was performed for insulin (red) and glucagon (brown). Magnification bar = 50 μm. β-Cell mass was calculated and changes are shown with age (days postinjection) in (e) for control (solid line) and STZ-treated (broken line) animals. Data are presented as mean $\pm$ SEM. $^{*}P < 0.05$, $^{\#}P < 0.01$ versus day 4 within group. $^{\S}P < 0.001$ versus control for each age

Localization and expression of VEGF and HGF

Immunofluorescent co-staining for insulin and VEGF within islets showed that approximately 90% of the insulin-immunoreactive cells also contained VEGF in both control and STZ-treated animals at all ages studied (Figure 5a). No VEGF presence was seen in other islet endocrine cell types, or in exocrine tissue. VEGF mRNA expression within the whole pancreata were measured by quantitative PCR between days 4 and 40, and expressed relative to that at day 4 (Figure 5b). In control animals VEGF mRNA levels increased steadily between days 8 and 40. In STZ-treated rats VEGF mRNA levels were significantly reduced versus controls at days 12 and 16, but were greater on day 20. This occurred despite the β-cell mass still being substantially less in STZ-treated animals on days 20 and 40.

Immunoreactivity for HGF was restricted to the vascular tissue of the islet in both control and STZ-treated rats, as shown by co-localization with BS-l (Figure 5c). Slight punctate staining was also observed in acinar cells. The expression levels of HGF mRNA in pancreas of control animals increased two- and three-fold at days 12 and 16, respectively, but then declined to barely detectable levels thereafter (Figure 5d). Levels of HGF expression were similar to controls in STZ-treated rats between days 4 and 12, but fell to low levels at day 16, significantly reduced compared with control animals ($P < 0.05$).

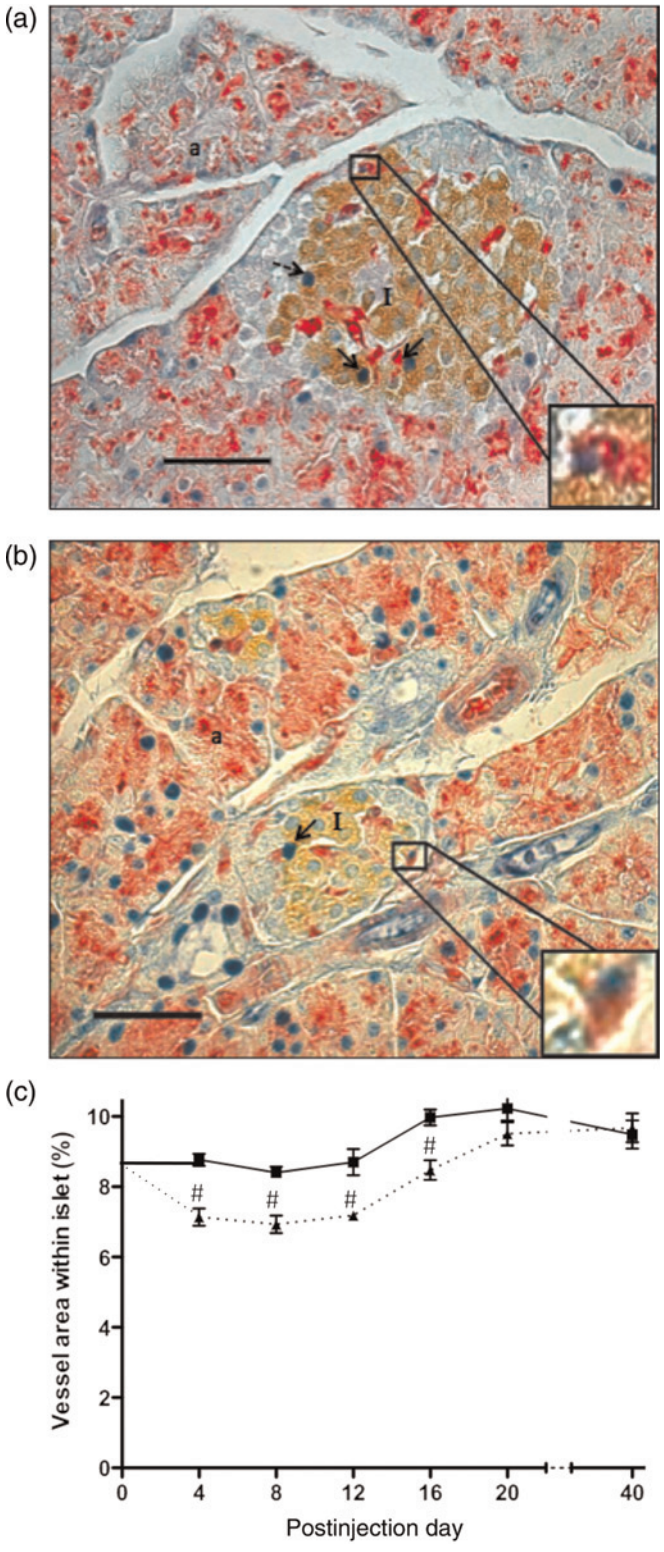

Figure 3 Representative morphology for an islet (I) from control animals (a) and from a streptozotocin (STZ)-treated animal (b) 16 days after treatment with STZ or saline. Immunohistochemistry was performed to visualize insulin (brown), endothelial cells using *Bandeiraea simplicifolia* lectin (BS-I) (red) and proliferating cell nuclear antigen (blue). Examples of proliferative endothelial cells are shown within the enlarged views, while examples of proliferating β-cells are shown with arrows. Magnification bar = 50 μm. The area within islets occupied by capillaries was calculated (c) for control rats (solid line) or those treated with STZ (broken line) between four and 40 days following treatment with STZ or saline. Data are presented as mean $\pm$ SEM. $^{\#}P <$ 0.01 versus control for same age

Table 2 Percentage of capillaries found within the core of the islet, as defined by being surrounded by insulin-immunopositive β-cells, for control rats or those treated with streptozotocin (STZ) between four and 40 days after treatment

	% Capillaries in islet core	
Day	Control	STZ
4	81 $\pm$ 4	50 $\pm$ 7*
8	77 $\pm$ 1	51 $\pm$ 5*
12	80 $\pm$ 1	51 $\pm$ 5*
16	79 $\pm$ 6	57 $\pm$ 7*
20	84 $\pm$ 3	58 $\pm$ 5*
40	86 $\pm$ 2	81 $\pm$ 5$^{\#}$

Values show mean $\pm$ SEM. n = 6–8 animals
$^{*}P < 0.001$ versus control same day
$^{\#}P < 0.001$ versus STZ day 4

Localization of islet extracellular matrix proteins

Collagen type IV was immunolocalized to the basement membrane surrounding the islets, but was also seen in association with intraislet blood vessels (Figure 6a) when these were identified in adjacent tissue sections using BS-l

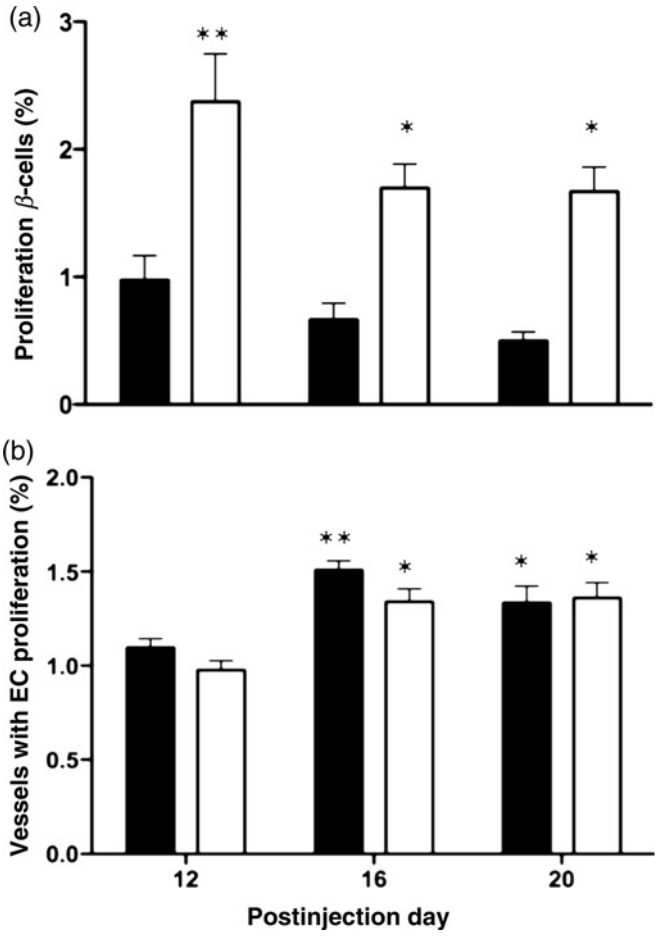

Figure 4 β-Cell and endothelial cell proliferation. The percent of β-cells that co-stained with proliferating cell nuclear antigen (PCNA) is shown in (a) for control animals (closed bars) or animals treated with streptozotocin (STZ) (open bars) at 12, 16 and 20 days following treatment. The percentage of islet capillaries that showed at least one PCNA-immunoreactive endothelial cell is shown in (b). Data are presented as mean $\pm$ SEM. $^{*}P < 0.05$, $^{**}P <$ 0.001 versus day 12 for either control or STZ (n = 5)

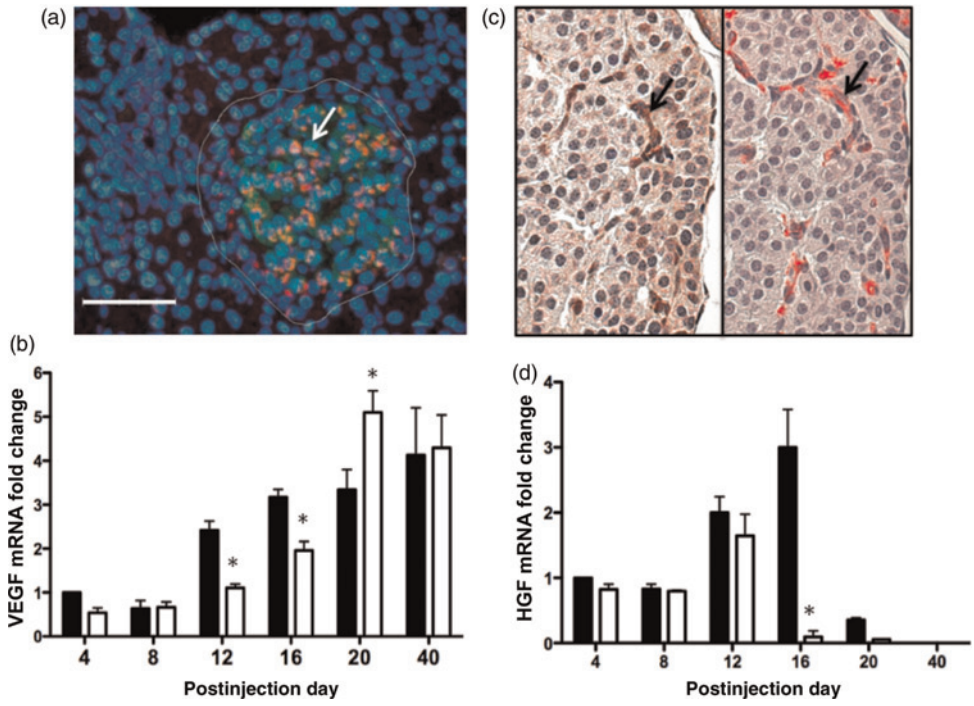

Figure 5 (a) Immunohistochemical co-localization of vascular endothelial growth factor (red) and insulin (green) within a representative islet (arrow, islet is circled in white), and (c) co-localization of hepatocyte growth factor (brown, arrow) within endothelial cells identified with BS-I lectin (red, arrow) in adjacent tissue sections. Sections were taken from a pancreas of a control-treated rat on day 16. Magnification bar = 50 μm. The ontogeny of vascular endothelial growth factor (VEGF) (b) or hepatocyte growth factor (HGF) (d) mRNA was measured in whole pancreas by realtime polymerase chain reaction between four and 40 days for control animals (closed bars) or animals that received streptozotocin (open bars). Data represent mean values ± SEM. $^{*}P < 0.05$ or better versus control values for the same day

lectin (Figure 6b). The relative intraislet area that was immunopositive for type IV collagen was calculated and shown to be approximately 10% in control animals at all ages examined (Figure 6c). In STZ-treated animals, the collagen-immunoreactive islet area was significantly lower than in control animals at all ages from days 4 to 40, consistent with the finding of a reduced area occupied by capillaries within the islets. Immunoreactivity for laminin within the islets showed a similar distribution to that of type IV collagen and was similarly reduced following STZ treatment (not shown).

Discussion

We and others have demonstrated that during the first 3–4 weeks of neonatal life there is substantial remodelling of the rodent islets[12,24] involving a loss of β-cells by apoptosis and their replacement with new β-cells deriving from both within the islets and by neogenesis at the pancreatic ducts. Partial ablation of β-cells using STZ at this time results in a partial regeneration of β-cell mass.[13] As confirmed here, a loss of 70% of β-cells resulted in only a transient hyperglycemia, followed by regeneration of β-cell mass. However, β-cell mass was still significantly less than in age-matched control rats 40 days following STZ, and glucose handling was relatively impaired following a glucose tolerance test. The replacement of β-cell mass following STZ occurs both from within islets and by neogenesis of new endocrine tissue from the pancreatic ducts.[14] Since the ductal tissue does not have an associated dense microvasculature, it was not possible to examine changes at this anatomical location following STZ as we were able to do for islets. Associated vascular changes may also support the development of new islets from pancreatic ducts, although the contribution of newly formed, small islets to glucose homeostasis following recovery from STZ is not known.

We found associated changes to the islet microvasculature following STZ treatment. The mean islet area occupied by capillaries was reduced by approximately 20% following STZ and only recovered to control values after 20 days. Since mean islet area is reduced following STZ, subsequent to the β-cell death, a corresponding reduction of capillary area would have yielded an unchanged percentage area within islets. The decreased mean area of islets occupied by vessels seen following STZ shows that the reduction in capillary presence was relatively greater than the change in size due to loss of β-cells. The altered morphology of the vascular compartment was particularly apparent in the islet core, where the percentage of capillaries found in this region following STZ was significantly reduced by approximately 40%, and did not recover until day 40. Thus, it appears that destruction of β-cells resulted in an associated relative reduction in vascular ECs, which did not recover for over three weeks.

Regeneration of β-cells following STZ was at least partly due to an increased rate of proliferation of those β-cells remaining in the islets relative to controls. Previous reports highlighted the importance of the physical juxtaposition of the vasculature for optimal proliferation as

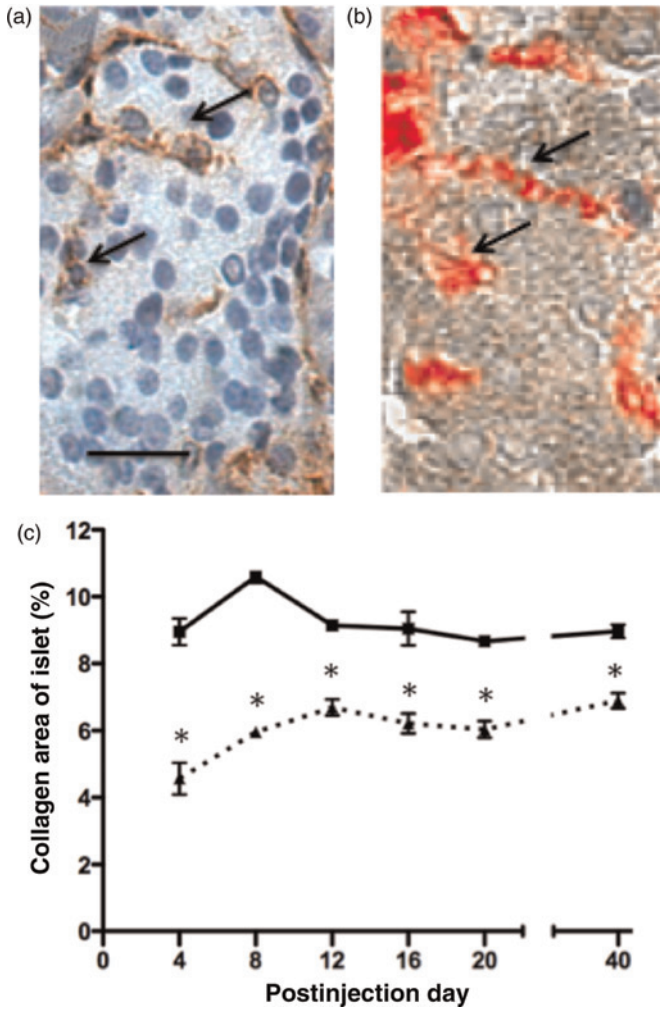

Figure 6 Immunohistological co-localization of type IV collagen (a) within an islet (brown, arrow) and of endothelial cells identified with BS-I lectin (red, arrow) (b) in an adjacent section of a control-treated rat on day 16. Magnification bar = 50 μm. The ontogeny of the percent intraislet area immunopositive for type IV collagen is shown (c) for control (solid line) and streptozotocin-treated animals (broken line) between four and 40 days. Data represent mean values $\pm$ SEM. $^{*}P < 0.05$ or better versus control

well as function of β-cells,[3] and that a re-structuring of the islet following damage may also require the recovery and re-organization of the vascular microenvironment.[4] VEGF, predominantly synthesized in the pancreas within the islets, and as shown here and by others, predominantly by the β-cells,[25] has been implicated as an angiogenic developmental trigger.[26] An increase in VEGF expression could signal an increase in the capillary density that could, in turn, provide a mitogenic stimulus to the β-cells.[27] VEGF mRNA within the pancreas of control rats steadily increased between chronological days 12 and 24, suggesting that the re-organization of the islet in the neonatal rat results in the appearance of β-cells in which VEGF is abundantly expressed. Following STZ treatment, the temporal rise in VEGF mRNA levels was delayed, but at day 20 postinjection, it actually exceeded that in pancreas of control rats. Since the β-cell mass at this time was only approximately half of that in controls, the expression of VEGF per β-cell must have been substantially elevated, but without a corresponding increase in vascular presence, and with no change in the frequency of EC proliferation. This might indicate that islet angiogenesis was blunted following STZ. VEGF expression in pancreas has been shown to be increased in situations of metabolic stress, as in the Zucker diabetic fatty (ZDF) rat model of type 2 diabetes, where an increase in the islet vascular density occurs prior to β-cell dysfunction.[28] VEGF expression has also been shown to be elevated in islets during hypoxia.[29] However, the expression of antiangiogenic peptides in pancreas, such as thrombospondin-1, has also been shown to be elevated in the ZDF rat, while thrombospondin-1-null mice have large, hypervascularized islets.[28,30] The source of thrombospondin-1 was shown to be the peripheral cells of the islets, perhaps α-cells.[30]

HGF is known to be produced by islet capillaries and bone marrow-derived endothelial precursor cells,[31,32] and promotes β-cell hyperplasia.[33,34] It is predominantly localized to the vasculature with a weak presence in acinar tissue, although its receptor, c-Met, is found on islet endocrine cells.[25] Pancreatic HGF mRNA transiently increased in abundance between two and three weeks of neonatal life and subsequently declined, as did the c-Met receptor as shown previously,[35] suggesting a role in β-cell developmental turnover, and islet remodelling. The disappearance with age of HGF expression from the vascular compartment may contribute to the reduced regenerative capacity of β-cells. Following STZ treatment, there was a premature loss of HGF expression at day 16, which could limit the extent of subsequent β-cell replacement. In this study, we measured VEGF and HGF mRNA levels in intact pancreas, rather than in isolated islets, because of the risk of substantial change in gene expression levels during islet isolation. It is likely that the pancreatic mRNA levels do reflect predominantly paracrine interactions within the islets, since no VEGF immunoreactivity was seen in exocrine tissue, and HGF presence was restricted to the islet microvasculature.

Intercommunication between the β-cell and vascular endothelium depends not only on locally expressed growth factors, but also on the integrity of the extracellular matrix.[2] This involves integrin signalling and key matrix components include type IV collagen and laminin.[36] Incubation of isolated rat islets with islet EC-conditioned culture medium increased β-cell insulin content and glucose-stimulated insulin release, effects that were abolished by the addition of a neutralizing antibody to the β1-chain of laminin.[37] The intraislet area occupied by immunoreactive type IV collagen was substantially reduced following STZ, consistent with substantial cellular remodelling and proteolytic modification of extracellular matrix. While the mean islet area occupied by microvasculature was initially depressed following STZ, it had recovered by day 20. However, this was not accompanied by a recovery of collagen presence, which was still relatively deficient. Hence, even when recovery of microvasculature had occurred, it may have been functionally deficient in facilitating β-cell growth and function due to altered extracellular matrix composition. Type IV collagen has previously been shown not to be required for basement membrane[38] or

capillary assembly,[39] but is required for optimal insulin release by β-cells in response to a glucose challenge.[15] The relative deficiency in collagen within the islets following STZ may reflect a functional immaturity of the reconstituted microvasculature with implications for β-cell function, and the persistence of glucose intolerance.

In summary, these results demonstrate that partial β-cell destruction by STZ is accompanied by a relative loss of microvasculature, particularly from the islet core. The subsequent generation of new β-cells by proliferation and their functional capacity is likely to be related to the recovery of the microvasculature involving the presence of growth factors such as HGF, and the reconstitution of the extracellular matrix. Both may be rate limiting to the recovery of β-cell mass following STZ insult in early life.

Author contributions: All authors participated in the design, interpretation of the studies, analysis of the data and review of the manuscript; MN and EA conducted the experiments, and DH and EA wrote the manuscript.

ACKNOWLEDGEMENTS

We would like to thank Brenda Strutt for her expertise and technical support, the animal care team for their assistance and Britt Nicholson for acting as a 'blinded' observer for histomorphological studies. This work was supported by the Canadian Institutes of Health Research (2005) and the Juvenile Diabetes Research Foundation (2003).

REFERENCES

1 Nikolova G, Strilic B, Lammert E. The vascular niche and its basement membrane. *Trends Cell Biol* 2007;**17**:19–25
2 Nikolova G, Lammert E. Interdependent development of blood vessels and organs. *Cell Tissue Res* 2003;**314**:33–42
3 Nikolova G, Jabs N, Konstantinova I, Domogatskaya A, Tryggvason K, Sorokin L, Fässler R, Gu G, Gerber HP, Ferrara N, Melton DA, Lammert E. The vascular basement membrane: a niche for insulin gene expression and beta cell proliferation. *Dev Cell* 2006;**10**:397–405
4 Olsson R, Carlsson P-O. The pancreatic islet endothelial cell: emerging roles in islet function and disease. *Int J Biochem Cell Biol* 2005;**38**:492–7
5 Yao VJ, Ozawa MG, Trepel M, Arap W, McDonald DM, Pasqualini R. Targeting pancreatic islets with phage display assisted by laser pressure catapult microdissection. *Am J Pathol* 2005;**166**:625–36
6 Johansson M, Mattsson G, Andersson A, Jansson L, Carlsson PO. Islet endothelial cells and pancreatic beta-cell proliferation: studies *in vitro* and during pregnancy in adult rats. *Endocrinology* 2006;**147**:2315–24
7 Yashpal NK, Li J, Wheeler MB, Wang R. Expression of β1 integrin receptors during rat pancreas development – sites and dynamics. *Endocrinology* 2005;**146**:1798–807
8 Bosco D, Meda P, Halban PA, Rouiller DG. Importance of cell–matrix interactions in rat islet beta-cell secretion *in vitro*: role of alpha6beta1 integrin. *Diabetes* 2000;**49**:233–43
9 Henderson JR, Moss MC. A morphometric study of the endocrine and exocrine capillaries of the pancreas. *Q J Exp Physiol* 1985;**70**:347–56
10 Schittny JC, Yurchenco PD. Basement membranes: molecular organization and function in development and disease. *Curr Opin Cell Biol* 1989;**1**:983–8
11 Konstantinova I, Lammert E. Microvascular develoment: learning from pancreatic islets. *BioEssays* 2004;**26**:1069–75
12 Scaglia L, Cahill CJ, Finegood DT, Bonner-Weir S. Apoptosis participates in the remodeling of the endocrine pancreas in the neonatal rat. *Endocrinology* 1997;**138**:1736–41
13 Portha B, Levacher C, Picon L, Rosselin G. Diabetogenic effect of streptozotocin in the rat during the perinatal period. *Diabetes* 1974;**23**:889–95
14 Thyssen S, Arany E, Hill DJ. Ontogeny of regeneration of beta-cells in the neonatal rat after treatment with streptozotocin. *Endocrinology* 2006;**147**:2346–56
15 Nir T, Melton DA, Dor Y. Recovery from diabetes in mice by beta cell regeneration. *J Clin Invest* 2007;**117**:2553–61
16 Wang RN, Bouwens L, Kloppel G. Beta-cell growth in adolescent and adult rats treated with streptozotocin during the neonatal period. *Diabetologia* 1996;**39**:548–57
17 Bonner-Weir S, Trent DF, Honey RN, Weir GC. Responses of neonatal rat islets to streptozotocin: limited B-cell regeneration and hyperglycemia. *Diabetes* 1981;**30**:64–9
18 Hasegawa Y, Ogihara T, Yamada T, Ishigaki Y, Imai J, Uno K, Gao J, Kaneko K, Ishihara H, Sasano H, Nakauchi H, Oka Y, Katagiri H. Bone marrow (BM) transplantation promotes beta-cell regeneration after acute injury through BM cell mobilization. *Endocrinology* 2007;**148**:2006–15
19 Hess D, Li L, Martin M, Sakano S, Hill DJ, Strutt B, Thyssen S, Gray DA, Bhatia M. Bone marrow-derived stem cells initiate pancreatic regeneration. *Nat Biotechnol* 2003;**21**:763–70
20 Lechner A, Yang YG, Blacken RA, Wang L, Nolan AL, Habener JF. No evidence for significant transdifferentiation of bone marrow into pancreatic beta cells *in vivo*. *Diabetes* 2004;**53**:616–23
21 Laitinen L. *Griffonia simplicifolia* lectins bind specifically to endothelial cells and some epithelial cells in mouse tissues. *Histochem J* 1987;**19**:225–34
22 Mattsson G, Carlsson PO, Olausson K, Jansson L. Histological markers for endothelial cells in endogenous and transplanted rodent pancreatic islets. *Pancreatology* 2002;**2**:155–62
23 Movassat J, Portha B. Beta-cell growth in the neonatal Goto–Kakisaki rat and regeneration after treatment with streptozotocin at birth. *Diabetologia* 1999;**42**:1098–110
24 Petrik J, Arany E, McDonald TJ, Hill DJ. Apoptosis in the pancreatic islet cells of the neonatal rat is associated with a reduced expression of insulin-like growth factor II that may act as a survival factor. *Endocrinology* 1998;**139**:2994–3004
25 Watanabe H, Sumi S, Kitamura Y, Nio Y, Higami T. Immunohistochemical analysis of vascular endothelial growth factor and hepatocyte growth factor, and their receptors, in transplanted rat islets. *Surg Today* 2003;**33**:854–60
26 Brissova M, Shostak A, Shiota M, Wiebe PO, Poffenberger G, Kantz J, Chen Z, Carr C, Jerome WG, Chen J, Baldwin HS, Nicholson W, Bader DM, Jetton T, Gannon M, Powers AC. Pancreatic islet production of vascular endothelial growth factor-A is essential for islet vascularization, revascularization, and function. *Diabetes* 2006;**55**:2974–85
27 Johansson M, Mattsson G, Andersson A, Jansson L, Carlsson PO. Islet endothelial cells and pancreatic beta-cell proliferation: studies *in vitro* and during pregnancy in adult rats. *Endocrinology* 2006;**147**:2315–24
28 Li X, Zhang L, Meshinchi S, Dias-Leme C, Raffin D, Johnson JD, Treutelaar MK, Burant CF. Islet microvasculature in islet hyperplasia and failure in a model of type 2 diabetes. *Diabetes* 2006;**55**:2965–73
29 Vasir B, Aiello LP, Yoon KH, Quickel RR, Bonner-Weir S, Weir GC. Hypoxia induces vascular endothelial growth factor gene and protein expression in cultured rat islet cells. *Diabetes* 1998;**47**:1894–903
30 Crawford SE, Stellmach V, Murphy-Ullrich JE, Ribeiro SM, Lawler J, Hynes RO, Boivin GP, Bouck N. Thrombospondin-1 is a major activator of TGF-β1 *in vivo*. *Cell* 1998;**93**:1159–70
31 Miyamoto Y, Suyama T, Yashita T, Akimaru H, Kurata H. Bone marrow subpopulations contain distinct types of endothelial progenitor cells and angiogenic cytokine-producing cells. *J Mol Cell Cardiol* 2007;**43**:627–35
32 Izumida Y, Aoki T, Yasuda D, Koizumi T, Suganuma C, Saito K, Murai N, Shimizu Y, Hayashi K, Odaira M, Kusano T, Kushima M, Kusano M. Hepatocyte growth factor is constitutively produced by donor-derived bone marrow cells and promotes regeneration of pancreatic beta-cells. *Biochem Biophys Res Commun* 2005;**333**:273–82
33 Garcia-Ocana A, Takane KK, Syed MA, Philbrick WM, Vasavada RC, Stewart AF. Hepatocyte growth factor overexpression in the islet of transgenic mice increases beta cell proliferation, enhances islet mass, and induces mild hypoglycemia. *J Biol Chem* 2000;**275**:1226–32

34 Dai C, Li Y, Yang J, Liu Y. Hepatocyte growth factor preserves beta cell mass and mitigates hyperglycemia in streptozotocin-induced diabetic mice. *J Biol Chem* 2003;**278**:27080–7

35 Calvo EL, Boucher C, Pelletier G, Morisset J. Ontogeny of hepatocyte growth factor and c-met/hgf receptor in rat pancreas. *Biochem Biophys Res Commun* 1996;**229**:257–63

36 Kaido T, Yebra M, Cirulli V, Montgomery AM. Regulation of human beta-cell adhesion, motility, and insulin secretion by collagen IV and its receptor alpha1beta1. *J Biol Chem* 2004;**279**:53762–9

37 Johansson A, Lau J, Sandberg M, Borg LA, Magnusson PU, Carlsson PO. Endothelial cell signalling supports pancreatic beta cell function in the rat. *Diabetologia* 2009;**52**:2385–94

38 Poschl E, Schlotzer-Schrehardt U, Brachvogel B, Saito K, Ninomiya Y, Mayer U. Collagen IV is essential for basement membrane stability but dispensable for initiation of its assembly during early development. *Development* 2004;**131**:1619–28

39 Thyboll J, Kortesmaa J, Cao R, Soininen R, Wang L, Livanainen A, Sorokin L, Risling M, Cao Y, Tryggvason K. Deletion of the laminin alpha4 chain leads to impaired microvessel maturation. *Mol Cell Biol* 2002;**22**:1194–202

(Received October 17, 2009, Accepted December 4, 2009)